

# 1 Muon track reconstruction and veto performance 2 with D-Egg sensor for IceCube-Gen2

---

## The IceCube Gen2 Collaboration

[http://icecube.wisc.edu/collaboration/authors/icrc17\\_gen2](http://icecube.wisc.edu/collaboration/authors/icrc17_gen2)

E-mail: [achim.stoessl@icecube.wisc.edu](mailto:achim.stoessl@icecube.wisc.edu)

The planned extension of IceCube, IceCube-Gen2, a cubic-kilometer sized neutrino observatory, aims at increasing the rate of observed astrophysical neutrinos by up to a factor of 10. The discovery of a high energy neutrino point source is one of its primary science goals. Improving the sensitivity of the individual modules is a necessity to achieve the desired design goal of IceCube-Gen2. A way of improving their sensitivity is the increase of photocathode area. The proposed module called the D-Egg will utilize two 8" Hamamatsu R5912-100 photomultiplier tubes (PMTs), with one facing upwards and one downwards. These PMTs have an increased quantum efficiency and their sensitivity is comparable to the 10" PMT used by IceCube. This essentially leads to an increase in sensitivity by almost a factor of 2 with a full  $4\pi$  solid angle acceptance. A simulation study is presented that indicates improvement in angular resolution using current muon reconstruction techniques due to the new sensor design. Since the proposed module is equipped with an upward facing PMT, further emphasis will be set on the development of new reconstruction techniques that exploit this geometry, as well as an improvement of veto probability for incoming muon tracks, which is crucial for neutrino astronomy in the Southern sky.

**Corresponding author:** A. Stoessl<sup>\*1</sup>

<sup>1</sup>*International Center for Hadron Astrophysics, Graduate School of Science, Chiba University 1-33, Yayoi-cho, Inage-ku, Chiba-shi, Chiba, 263-8522 JAPAN*

*35th International Cosmic Ray Conference -ICRC2017-  
10-20 July, 2017  
Bexco, Busan, Korea*

---

\*Speaker.

3 **1. IceCube Gen2**

4 The IceCube neutrino observatory at the geographic South Pole is a cubic kilometer array of  
 5 photosensors which is able to detect the faint Cherenkov light produced by secondaries from inter-  
 6 actions of neutrinos with the glacial ice [1]. So far, the experiment has yielded a plethora of science  
 7 results, among them the discovery of a neutrino flux most likely of extraterrestrial origin [2]. After  
 8 6 years of data-taking, with the completed detector, a precise measurement of the extraterrestrial  
 9 neutrino flux is still limited by statistics. To overcome the statistical limitations and to improve the  
 10 effective area for neutrino events in the energy regime beyond 10 PeV as well as the point source  
 11 sensitivity, an extension of the IceCube array has been proposed [4]. The proposed geometry for  
 12 IceCube-Gen2 considered in this work is shown in Figure 1. The geometry shows a larger exten-  
 13 sion in the x-y plane than in depth. It is optimized for the reconstruction of horizontal muon tracks,  
 since these have the highest contribution to the point-source sensitivity [5].

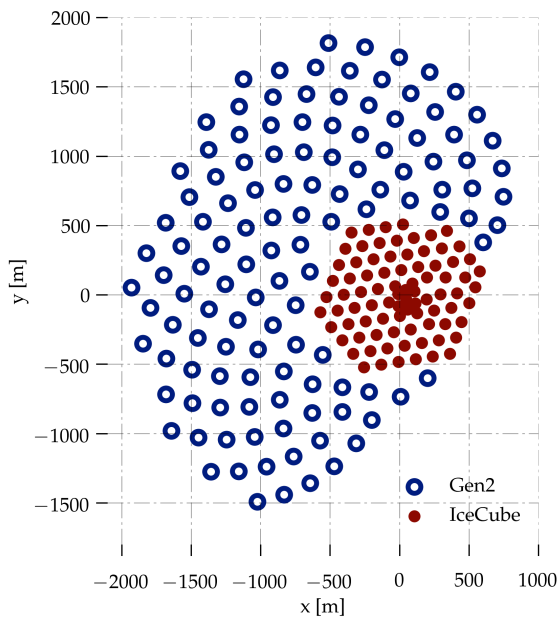


**Figure 1:** A proposed geometry for IceCube-Gen2 which is used for this study. In addition to the 86 strings of IceCube, which can be seen as the hexagonal shape marked with the red dots, 120 new strings with each 80 sensors are arranged in a complex grid geometry to optimize the veto power for incoming muon tracks. The average distance between the new strings is about 240 m with a vertical spacing between individual sensors of 17 m. The extension of IceCube to larger positive x-values is prohibited due to the runway of the South Pole Station.

14  
 15 **2. The D-Egg sensor for Gen2**

16 Several different sensor designs for IceCube-Gen2 are under investigation. However relevant  
 17 for this study are the following two proposed designs:

- 18 ▶ The PDOM [7], which is basically the same design as the IceCube optical sensor[6], however  
 19 with a PMT with a higher quantum efficiency. It features a single 10" PMT which is facing  
 20 downwards and a improved readout.
- 21 ▶ The D-Egg [8], which follows the design of the PDOM, however includes another PMT  
 22 facing upwards. The PMTs are 8", so the total diameter of the D-Egg is slightly smaller than  
 23 the PDOM and it has about 1.48 more photocathode area than the PDOM for a Cherenkov  
 24 weighted spectrum.

25 Due to high drill costs at the South Pole, it is desirable to deploy sensors with a large photocathode  
 26 area to keep the cost for the average  $\text{cm}^2$  photocathode as low as possible. The high drill costs can  
 27 be reduced by drilling holes with a smaller diameter. As the diameter of the D-Egg is 10% smaller  
 28 than the diameter of the PDOM, about 20% of the fuel cost can be saved during deployment. A  
 29 graphic of the D-Egg with its dimensions is shown in Figure 2. The two Hammaatsu R5912-100  
 30 high quantum efficiency PMTs are enclosed in a highly transparent glass housing, which is opti-  
 31 mized for transparency in the near ultraviolet. The high voltage for the PMTs is generated on two  
 32 boards, and the final design will feature a board for readout electronics as well. In this proceed-  
 33 ing, we investigate the performance of the D-Egg using several existing reconstruction methods  
 developed for IceCube and compare the results against the benchmark PDOM performance.

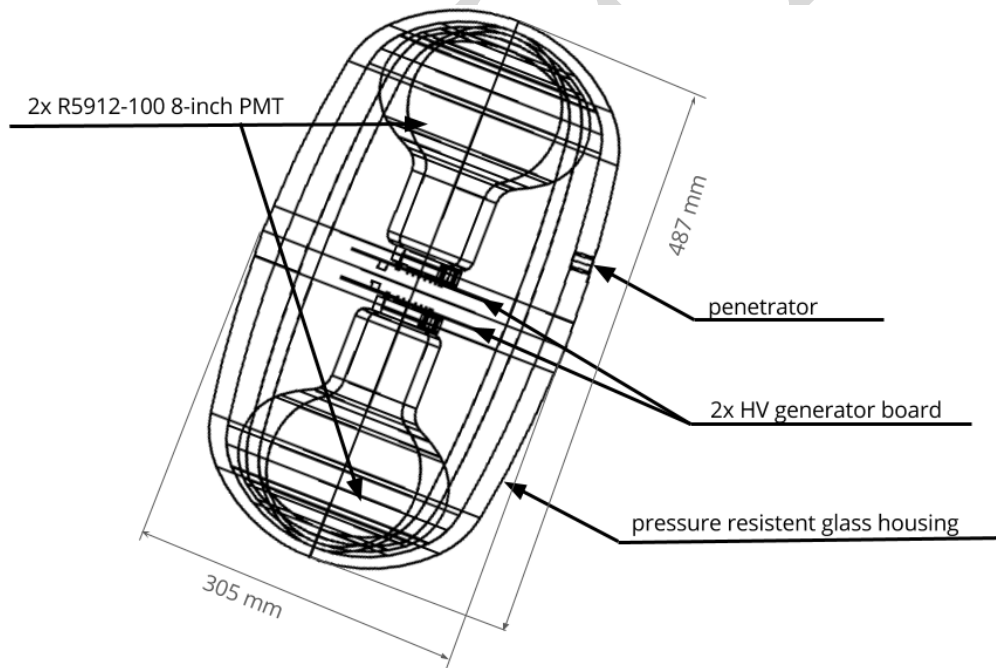


**Figure 2:** A schematic of the D-Egg design. It features two 8" PMTs enclosed in a highly transparent glass housing, Its diameter is 10% smaller then that of the current IceCube optical module.

34

### 35 3. Simulation

36 We simulated muons from an  $E^{-1.4}$  power-law spectrum in the energy range of 10 TeV to 10  
 37 PeV with a full  $4\pi$  angular distribution. The muons were injected at a cylindrical surface enclosing  
 38 the detector and then propagated through the ice. The light emerging by stochastic energy losses  
 39 of the muons as well as the smooth Cherenkov light were simulated and the photon propagation is  
 40 handled by the direct propagation code developed for IceCube. The simulation features a bulk ice  
 41 model which means that the ice is homogenous throughout the detector. As the direct propagation  
 42 of photons is computationally consumptive, the detector simulation for D-Egg and PDOM are  
 43 sharing the same photon simulation as input, which means that the photons have been simulated  
 44 once and then the simulation branches into the different types of detector simulation. To further

45 increase the simulation efficiency, several simplifications were made. The effects of glass and gel  
 46 and the module geometry are not simulated individually. Instead the photons are weighted with  
 47 the angular sensitivity of the module as well as the wavelength dependent quantum efficiency. The  
 48 efficiency of the photocathode is assumed to be constant over the whole area. To further increase  
 49 the efficiency of the simulation, the size of the modules is scaled up and the number of propagated  
 50 photons is decreased accordingly.  
 51 The noise introduced by the PMT and the glass housing is simulated in the same way for D-Egg  
 52 and PDOM, however with absolute values scaled by the photocathode area. Further simplifications  
 53 are made in the PMT and sensor simulation. The PMT simulation is done as for the PMT used in  
 54 IceCube, as they are very similar in their behavior. The benefit of this is that the same simulation  
 55 chain can be used for D-Egg as well as for the IceCube DOM and PDOM. As the readout electronics  
 56 for the D-Egg is not yet finalized, we assume a perfect readout with an infinitesimal small binning  
 in time. The IceCube array, as part of IceCube-Gen2 has been simulated to our best knowledge.

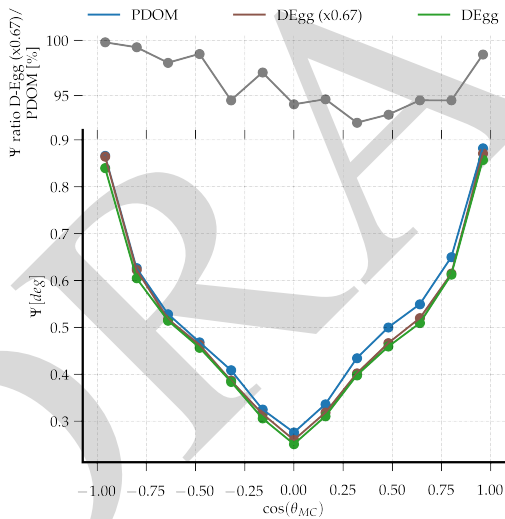


**Figure 3:** The results of the SPEFit reconstruction for both sensors, D-Egg and PDOM binned in the cosine of the simulated muon direction. The D-Egg effective area is scaled down by a factor of 0.67 to match the PDOM effective area. Muons with a cosine of -1 are entering the detector from below, those with 1 from above respectively.

57

#### 58 4. Muon reconstruction

59 The simulated dataset was reconstructed with a set of algorithms. In this study we focus on  
 60 the reconstruction algorithms SPEFIT and SPLINE-RECO [9]. The algorithms operate on the  
 61 reconstructed pulses, each using a different method. While SPEFIT uses a simple analytical ice-  
 62 model and a likelihood with one term per optical module, where only the first registered pulse  
 63 is considered, SPLINE-RECO is capable of constructing a likelihood with a probability density  
 64 function (pdf) obtained from tabulated values, and thus is able to also include more complicated  
 65 models for the glacial ice. To compare the accuracy of the reconstruction results, we looked at the  
 66 distributions of the opening angle  $\Psi$  between the simulated and reconstructed track. The median  
 67 of this distribution is used as a Figure of merit. No quality cuts have been applied, yet we restrict  
 68 ourself to tracks which traverse the instrumented volume.

69 We aim to investigate the impact of the increased photocathode area and segmentation on the re-  
 70 construction independently. As such, we work with different types of D-Egg simulation:

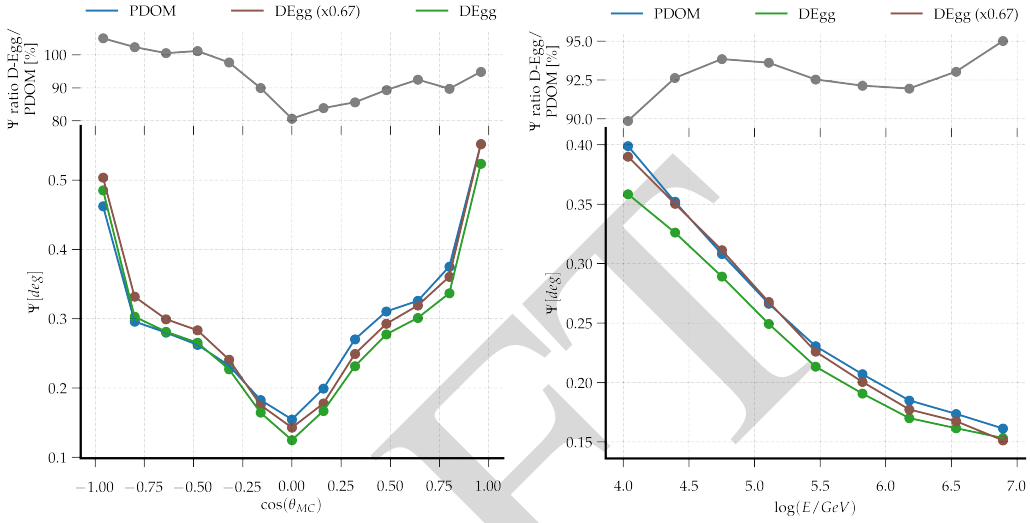


**Figure 4:** The results of the reconstruction SPLINE-RECO, binned in the cosine of the simulated muon direction on the left and binned in the logarithm of the muon energy on the right. Muons with a cosine of -1 are entering the detector from below, those with 1 from above respectively.

- 71     ▶ Simulation of the D-Egg “as is” as described in section 3.
- 72     ▶ The same as above, however the effective photocathode area is scaled down by a factor of
- 73         0.67 to match the photocathode area of the PDOM
- 74     ▶ Simulation of the D-Egg where either the upward or downward facing PMT is disabled.

75 All types of simulations share the same simulated photons, but then branch in different detector  
 76 simulations. First, the behavior of the two individual PMTs is studied. As the simulation has up-  
 77 down symmetry, we expect the same performance for the datasets with only pulses in the upper or  
 78 lower PMT. The results for the SPEFIT reconstructions is shown in Figure 3. All reconstructions  
 79 perform best for more horizontal events due to the fact that the Gen2 geometry is elongated more  
 80 in the x and y dimension than in the z dimension. This means that horizontal tracks cross a larger  
 81 instrumented volume. Also as the string spacing is 240 m, vertical tracks have a lower light yield  
 82 if they enter the detector in between strings. For upward-going muons, if only the lower PMT of  
 83 D-Egg is used as reconstruction input, it can be seen that the performance is slightly better than  
 84 for the upper PMT only, and vice versa for downward going muons. The SPEFIT reconstruction  
 85 yields a higher accuracy for the D-Egg sensor, which we quantify to be about 5% in the horizontal  
 86 and downward region due to the segmentation of the D-Egg only as we here compare to the scaled-  
 87 down version. We attribute this to the fact that SPEFIT uses only the first pulse recorded by each  
 88 PMT, and the doubling of PMT thus increases the number of pulses available to the reconstruction,  
 89 especially for the downward region.

90 The performance SPLINE-RECO of the reconstruction is shown in Figure 4. The D-Egg exhibits  
 91 up to 15% higher accuracy in reconstruction especially in the horizontal region, which is important  
 92 to point source searches [5]. The reconstruction in the downward going region yields more accurate  
 93 results with D-Egg as well. Comparing the results as a function of the true muon energy  $E_{MC}$  as it

94 is shown in the right panel of Figure 4, the SPLINE-RECO reconstruction gains for D-Egg due to  
 95 the higher photoelectron (PE) yield. However it seems that most of the gain results from the larger  
 96 photocathode area of D-Egg.

## 97 5. Likelihood improvements for segmented sensors

Figure 4 shows that the increase in reconstruction performance for the D-Egg seems to be attributed mostly to its larger total photocathode area. Thus, we investigate the details of the SPLINE-RECO reconstruction. Developed for IceCube, the here used likelihood is not optimized for segmented sensors, and thus it does not exploit their full potential. The likelihood is given by [9]:

$$L = \prod_{j=1}^{N_{DOM}} N \cdot p_j(t_j) \cdot (1 - P_j(t_1))^{N-1} \quad (1)$$

98 In the above equation,  $N$  stands for the number of hits on a certain optical module,  $p_j$  and  $P_j$  are  
 99 the time residual pdf and cumulative density function for the hit DOM and  $t_j$  is the time of the  
 100 first hit of the given DOM. Contours of this likelihood function can be seen in Figure 5. This  
 101 simplified example illustrates the likelihood space for a single module, placed in the middle of the  
 102 individual figures. A muon track crosses the plane of the figure orthogonal in 120 m distance. In  
 103 this example, the sensor detects 20 photo electrons with arrival times given by the time residual pdf.  
 104 The  $1\sigma$  contour for the likelihood developed for the IceCube DOM is shown with the two circles  
 105 with the red color. As it can be seen, the direction of the individual PMT imposes only very small  
 106 constraints on the red likelihood contour. As a reason, we suspect the importance of the late photo  
 107 electrons in the arrival time distribution. In the current approach, the likelihood is constructed by  
 108 the use of the timing of the first photo electron and the number of total hits, but does not account for  
 109 the timing of later photo electrons. Extending equation 1 to include the arrival times of all photo  
 110 electrons can improve the likelihood. This new likelihood is illustrated in the example in Figure 5  
 111 with the blue contours. It allows for a more precise determination of the track position, which in  
 112 total will most likely lead to a better angular resolution of the overall reconstruction algorithm. The  
 113 IceCube-Gen2 collaboration is currently working on a reconstruction implementing this approach.

## 115 6. Veto performance

116 An effective method to select an all flavor neutrino sample with high purity and full sky accep-  
 117 tance is the implementation of a veto: Using the outer strings and top and bottom layer of optical  
 118 modules, incoming muon tracks can be tagged and removed from such a sample. The method has  
 119 been proven successful and lead to the discovery of the extraterrestrial neutrino flux [2].

120 The method has been applied and studied for IceCube-Gen2 [10]. In the context of this proceed-  
 121 ings we are investigating the impact of D-Egg on the efficiency of the veto algorithm. An important  
 122 parameter of the current algorithm is the veto threshold, which is the charge required in the veto  
 123 region to trigger the veto, which is currently set to 3 PEs. Since the D-Egg has an upward facing  
 124 PMT, we expect a higher performance for downward going cosmic ray muon tracks. Due to the  
 125 D-Eggs larger photo cathode, we also expect a higher probability to detect charge in the veto region



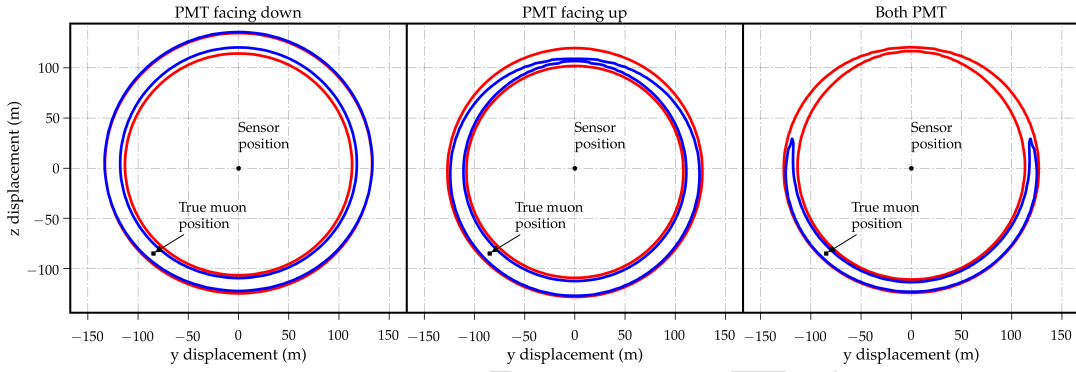


**Figure 5:** Likelihood contours of two different likelihoods for a single D-Egg sensor in case of a muon traversing the plane in orthogonal direction. The red contour results from the likelihood used in SPLINE-RECO, the blue contour is a proposed likelihood considering the timing of the late pulses in the arrival time distribution. On the left, the contours are shown for the lower PMT only. The contours are based on an Asimov sample. The middle plot shows the situation for the upper PMT and on the right the combined contours of both PMTs are shown.

126 at all. This is illustrated in Figure 6: The distribution of collected charge for the upper 2 layers of  
 127 modules of the IceCube-Gen2 geometry results in a higher probability to veto incoming muons. Further impact of the use of D-Eggs in the veto region is currently under investigation.

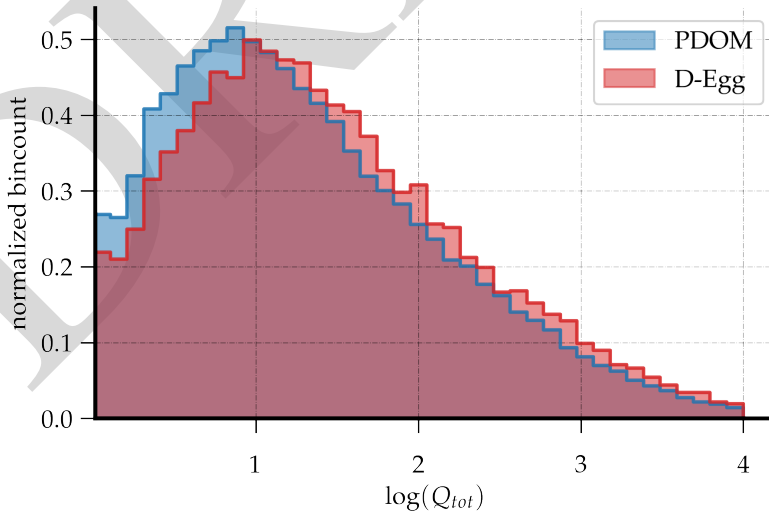


**Figure 6:** The collected charge in the upper layer of the IceCube-Gen2 array. The collected charge is shown for the uppermost 2 layers of optical modules.

128

## 129 7. Summary

130 For the first time, we present a study of muon track angular resolutions with current  
 131 reconstruction techniques used by IceCube for the proposed extension IceCube-Gen2. We  
 132 compare a new sensor design, the D-Egg, to an improved sensor based on the current IceCube  
 133 design (PDOM). The angular resolution for common reconstruction algorithms in IceCube were  
 134 studied for both sensors with a full-sky muon simulation and we find an improvement of the  
 135 angular resolution of D-Egg of about 20% compared to PDOM. The major part of the

136 improvement can be attributed to the larger photo cathode area of D-Egg. Investigating the fact  
137 that segmentation of the sensors seems to have only a small impact on the reconstruction result,  
138 we find that there are no existing reconstruction methods that fully take advantage of the module  
139 segmentation. Efforts are ongoing to develop a reconstruction that more accurately incorporates  
140 late photon timing information, and thus exploits all of the information provided by the D-Egg  
141 module. Besides the improvement in angular resolution, we show that the veto performance for  
142 the current implementation of the IceCube veto can be improved by using D-Eggs as well. We  
143 studied the deposited charge in the upper layer of the IceCube-Gen2 array and find a significant  
144 increase in the low charge region around the 3 PE threshold. In conclusion, we find that we are  
145 on a good track to improve the current IceCube reconstruction and veto techniques to exploit the  
146 full potential of new approaches in sensor design for IceCube-Gen2 and encourage further, more  
147 detailed studies to follow.

## 148 References

- 149 [1] **IceCube** Collaboration, A. Achterberg et. al., *APP* **26** (2006) P155-173.  
150 [2] **IceCube** Collaboration, M.G. Aartsen et. al., *SCI* **342(6161)** (2006) P1242856.  
151 [3] **IceCube** Collaboration, M.G. Aartsen et. al., *PRL* **131** (2014) P101101.  
152 [4] **IceCube** Collaboration, M. G. Aartsen et al., *astro-ph/1412.5106* (2014).  
153 [5] **IceCube-Gen2** Collaboration, [PoS \(ICRC2017\) 991](#) (these proceedings).  
154 [6] K. Hanson and O. Tarasova, *NIM* **567(1)** (2006) P214-217  
155 [7] **IceCube-PINGU** Collaboration, P. Sandstrom, *AIP* **1630(1)** (2014) P180-183.  
156 [8] **IceCube-Gen2** Collaboration, [PoS \(ICRC2017\) 1051](#) (these proceedings).  
157 [9] **AMANDA** Collaboration, J. Ahrens et al., *NIMA* **524** (2004) P169-194.  
158 [10] **IceCube-Gen2** Collaboration, [PoS \(ICRC2017\) 945](#) (these proceedings).